Comparison of Iron-59, Indium-111, and Gallium-69 Transferrin as a Macromolecular Tracer of Vascular Permeability and the Transferrin Receptor

Hideo Otsuki*, Arturo Brunetti†, Ernest S. Owens, Ronald D. Finn‡, and Ronald G. Blasberg

Nuclear Medicine Department, Warren G. Magnuson Clinical Center, National Institutes of Health, Bethesda, Maryland

Tracer amounts of [$^{59}Fe^{++}$]citrate, [$^{111}In^{+++}$]chloride, and [$^{68}Ga^{+++}$]chloride were complexed with autologous plasma transferrin. Each of these complexes were co-administered with [^{125}I] albumin by i.v. injection and their biodistribution was studied in Wistar rats. The plasma clearance of ^{59}Fe and [^{125}I]albumin was monoexponential with half-times of 49–70 and 277 min, respectively. The plasma clearance of ^{68}Ga and ^{111}In was biexponential with second component half-times of 157 and 232 min, respectively. Indium-111 tissue distribution was similar to that of [^{125}I]albumin in heart, lung, muscle, brain and Walker-256 allograft. Iron-59 distribution spaces were generally the highest of the metal complexes in all tissues except muscle, where the ^{68}Ga space was highest. The effects of transferrin-specific receptor-mediated endocytosis can be avoided in many organs and Walker-256 allografts by using the indium-transferrin complex, and the radiolabeled complex may be a convenient macromolecular tracer to estimate vascular permeability and vessel pore size in tumor and systemic tissue. In contrast, the iron-transferrin complex may be useful for measuring and imaging transferrin-specific receptors in brain and tumor tissue.

J Nucl Med 30:1676–1685, 1989

In search of a convenient macromolecular tracer to estimate vascular permeability and pore size in tumor and systemic tissues using positron emission tomography (PET), we studied the in vivo stability of various transferrin complexes. Iron, indium, and gallium ions are known to complex tightly with plasma transferrin and iron-52 (^{52}Fe) ($T\frac{1}{2}$ = 8.3 H), indium-110 (^{110}In) ($T\frac{1}{2}$ = 66 min) and gallium-68 (^{68}Ga) ($T\frac{1}{2}$ = 68 min) are positron-emitting radionuclides that can be produced and used in PET studies. Transferrin is a glycoprotein with a molecular weight of 80,000 D. The molecular size and aqueous diffusion constant of transferrin is similar to albumin (MW: 68,000 D) and immunoglobulin fragments Fab (MW: 50,000 D), and $F(ab')_2$. The hydrodynamic diameter of transferrin and albumin is ~6 nm (*1,2*). The axial length of IgG, Fab and $F(ab')_2$ is 13, 7, and 9 nm, respectively, and the hydrodynamic diameter is usually smaller than the axial length. The aqueous diffusion constant of transferrin, albumin, and IgG at 37.0°C is 6.2, 6.1, and 3.8×10^{-7} cm^2/sec, respectively (*1,2*). The transcapillary flux of transferrin could provide useful information related to vascular pore size in tumor and systemic tissues (*3*) that would directly bear on the transcapillary flux and delivery of immunoglobulin and immunoglobulin fragments to tumor tissue.

Radioiodinated human serum albumin has been used in clinical and experimental investigations of abnormal capillary permeability. However, positron emitting metal chelates of transferrin are more readily produced than carbon-11- (^{11}C)-labeled albumin or other macro-

Received Sept. 26, 1988; revision accepted June 21, 1989.

For reprints contact: Ronald G. Blasberg, MD, Nuclear Medicine Department, National Institutes of Health, Bldg. 10, Room 1C-41, Bethesda, MD 20892.

* Present address: Department of Neurosurgery, Osaka University Medical School, 1-1-50, Fukushima, Fukushima-ku, Osaka 553, Japan.

† Present address: Medicina Nucleare, Cancer Institute and 2nd Medical School, Naples, Italy.

‡ Present address: Nuclear Medicine Service, Memorial Sloan-Kettering Cancer Center, 1275 York Ave., New York, NY 10021.

molecules and the metal radionuclides have longer physical half-lives than [^{11}C]carbon. This latter point may be important for the study of low rates of transcapillary flux (*4*).

Radiolabeled metal chelates of transferrin have been shown to be useful macromolecular tracers in nuclear medicine. For example, [^{113m}In]- and [^{68}Ga]transferrin have been used to measure pulmonary vascular permeability (*5,6*) and indium chloride has been shown to be a sensitive and specific marker for abscess and chronic osteomyelitis which is in part the result of increased capillary permeability to the indium-transferrin complex that is associated with these conditions (*7,8*). It is also recognized that transferrin-metal chelates are suboptimal in certain applications, and there is no agreement about the stability of the transferrin-metal chelate in vivo (*4*).

The purpose of this paper was to test and compare the in vivo stability of three metal chelates of transferrin to that of albumin in the rat. From this comparison we have identified a potentially useful transferrin-metal chelates for studying systemic organ and tumor vascular permeability. In addition, we demonstrate tumor and organ specific differences with respect to the distribution of the three metal complexes in vivo, that in part probably reflects differences in affinity to the transferrin receptor between the three metal-transferrin chelates.

MATERIALS AND METHODS

Materials

Carrier free [^{111}In^{+++}]chloride, generator produced [^{68}Ga^{++}] chloride and [^{59}Fe^{++}]citrate (25 mCi/mg iron) were obtained from New England Nuclear, Boston, MA and [^{125}I]human serum albumin (0.8 mg albumin/ml; 6.8 μCi [^{125}I]albumin/ml) was obtained from Mallinckrodt, Inc., St. Louis, MO. Male Wistar rats (Charles River Farms, Wilmington, DE), weighing 250–350 g, were fed a standard Purina laboratory chow diet ad lib.

We studied five different transferrin-metal preparations in nine experimental sets (Table 1). In the first series of experiments, three ^{59}Fe preparations were studied; [Fe1] 1.1 MBq (30 μCi) [^{59}Fe^{++}]citrate in 30 μl was mixed with 1 ml phosphate buffer in pH 7.0; [Fe2] 1.1 MBq (30 μCi) [^{59}Fe^{++}]citrate in 30 μl was mixed with 1 ml normal saline solution; [Fe3] 1.1 MBq (30 μCi) [^{59}Fe^{++}]citrate in 30 μl was mixed with 1 ml plasma obtained from male Wistar rats and stored for no longer than 6 hr. The preparation of the metal-transferrin complex in the second series of experiments was performed as follows: the [Fe] preparation was the same as [Fe3] described above; [In] 1.8 MBq (50 μCi) ^{111}In+++-chloride in 1–2 μl was mixed with 1 ml rat plasma; [Ga] 2.6 MBq (70 μCi) [^{68}Ga^{+++}]chloride in 100 μl was also mixed with 1 ml rat plasma resulting in a plasma metal-transferrin complex. The final pH of these preparations was always between 7.0 and 7.5 except for [Fe2] (pH ≤ 6.0). Each of the above preparations also contained 0.15–0.19 MBq (4–5 μCi) [^{125}I]albumin that served as a reference macromolecule comparable in size to transferrin (Table 1) and each preparation represents a single dose per animal.

TABLE 1
Experimental Sets

Isotope	Diluent	Experiment duration	n	Abbreviation
[^{59}Fe]citrate [^{125}I]albumin	Phosphate buffer pH 7.0	120 min	7	[Fe1]
	Normal saline	120 min	5	[Fe2]
	Plasma	120 min	8	[Fe3]
[^{59}Fe]citrate [^{125}I]albumin	Plasma	120 min 30 min	8 5	[Fe]
[^{111}In]citrate [^{125}I]albumin	Plasma	120 min 30 min	8 7	[In]
[^{68}Ga]chloride [^{125}I]albumin	Plasma	120 min 30 min	5 5	[Ga]

Isotopes were complexed with plasma transferrin at room temperature.

The protein-bound fraction of ^{59}Fe, ^{111}In, ^{68}Ga, and ^{125}I was determined by ultrafiltration using an Amicon micropartition system (Amicon Corp., Danvers, MA); the micropartition membrane retains more than 99% of molecules over 30,000 D. Approximately 50 μl of plasma was added to the micropartition tubes and they were centrifuged for 15–20 min at 1500 *g* in a fixed angle clinical centrifuge. Twenty microliters of ultrafiltrate was counted and the nonfiltered or retention fraction (f_r) was calculated by:

$$f_r = 1 - (Cu/Cp), \quad (1)$$

where Cu and Cp are the concentrations in ultrafiltrate and plasma, respectively.

Animal Preparations

Brain tumors were produced in male Wistar rats by the injection of 10^5 Walker-256 mammary carcinoma cells into the right frontal lobe as previously described (*9*). Experiments were carried out 6 to 7 days after inoculation of the tumor cells when the intracerebral tumors were 3 to 4 mm in diameter. No rats showed signs or symptoms of the intracerebral tumor.

The animals were anesthetized with a halothane, nitrous oxide and oxygen gas mixture (2.0/40/60; v/v/v). Bilateral femoral artery and vein catheters were placed and a single extracorporeal arteriovenous shunt was formed on the right side to facilitate arterial sampling. The animals were allowed to recover from anesthesia for at least 2 hr. Rectal temperature was continuously monitored with a thermistor and maintained at 37°C using a heat lamp. The left femoral artery was connected to a pressure transducer for monitoring mean arterial blood pressure throughout the experiment. Arterial blood gases were measured just prior to the experiment (Radiometer, Copenhagen, Denmark).

Experimental Procedure

Biodistribution studies were performed in nine sets of Wistar rats bearing an intracerebral tumor (Table 1). Arterial

blood samples (0.1 ml) were drawn at 1, 3, 10, 30, 60, 90, and 120 min and plasma radioactivity was determined. An additional 0.1 ml of blood was removed at 1, 10 min, and the time of decapitation for the measurement of whole blood radioactivity and for ultrafiltration of the plasma sample. Evans blue solution (2% in saline) was injected (0.8 cc) 30 min before the end of the experiment to identify the intracerebral location of the Walker-256 allograft. Rats were killed at 30 or 120 min and tissue samples were rapidly obtained from various organs. The intracerebral tumor allograft was identified by Evans blue stained tissue. Brain samples were dissected from the tumor-free left side of the brain. All tissue samples were blotted on filter paper moistened with 0.9% NaCl to remove adhered blood. Sample radioactivity was measured in a Packard model 5650 gamma spectrometer with appropriate decay, background and crossover corrections.

Calculations

The plasma clearance of radioactivity for each experimental animal was evaluated and the apparent half-lives were determined for a single or biexponential components. The concentrations of ^{59}Fe, ^{111}In, ^{68}Ga, and ^{125}I in a unit mass of red blood cells (C_{rbc}) at 1, 10 min and the end of the experiments (30 or 120 min) were determined from:

$$C_{rbc} = 100\ (C_b - C_p\ (1 - Hct/100))/Hct, \qquad (2)$$

where C_b or C_p is the radioactivity in whole blood or plasma, respectively (cpm/ml), and Hct is the conventionally determined hematocrit for a sample of whole arterial blood. The distribution space (DS) of the radioisotope in the tissue was defined as:

$$DS = A_m/C_p \qquad (3)$$

where A_m is the measured radioactivity in the tissue (cpm/g), and C_p is the plasma activity at the time of decapitation (cpm/ml).

In normal brain regions the apparent increase in the iron distribution space was corrected for by the amounts of iron incorporated into red blood cells. The albumin space in the brain was assumed to represent the plasma volume, since albumin crosses the normal blood-brain barrier at a very slow rate (*10*) and [^{125}I]albumin could be assumed to remain almost totally within the intravascular space of the brain. To facilitate the comparisons, the distribution spaces of iron, indium and gallium were divided by the concurrently measured albumin space obtained in each animal (DS(metal)/DS(albumin)).

The metal and albumin distribution space values were compared within each experimental set using a paired t-test, and for comparisons between independent groups of rats, an unpaired t-test was used with appropriate estimates of variability and corresponding degrees of freedom.

RESULTS

Protein binding

Ultrafiltration was performed on each preparation. The nonspecific retention fraction [Eq. (1)] of each of the radioisotope solutions used in the preparations—[$^{59}Fe^{++}$]citrate, [^{111}In]chloride and [^{68}Ga]chloride—to the ultrafiltration membrane was 0.05 ± 0.01, 0.05 ± 0.01 and 0.15 ± 0.02 (mean ± s.d.), respectively. The retention fraction of the [Fe1] and [Fe2] preparations was 0.05 ± 0.01 and 0.05 ± 0.01, respectively. Our results confirmed previously reported data (*11,12*) indicating that iron, indium, and gallium in tracer amounts were quickly and almost completely bound to plasma proteins or formed macromolecular aggregates. The retention fraction of the [Fe3], [Fe], [In], and [Ga] preparations was 0.99 ± 0.01, 0.99 ± 0.01, 0.95 ± 0.02, and 0.86 ± 0.10, respectively. The retention fraction of [^{125}I]albumin was always more than 0.98.

Biodistribution

The mean arterial pressure for all animals was between 90–110 mmHg; arterial pO_2, pCO_2 and pH were 96 ± 8 torr, 34.2 ± 2.2 Torr, and 7.40 ± 0.05 (mean ± s.d.), respectively.

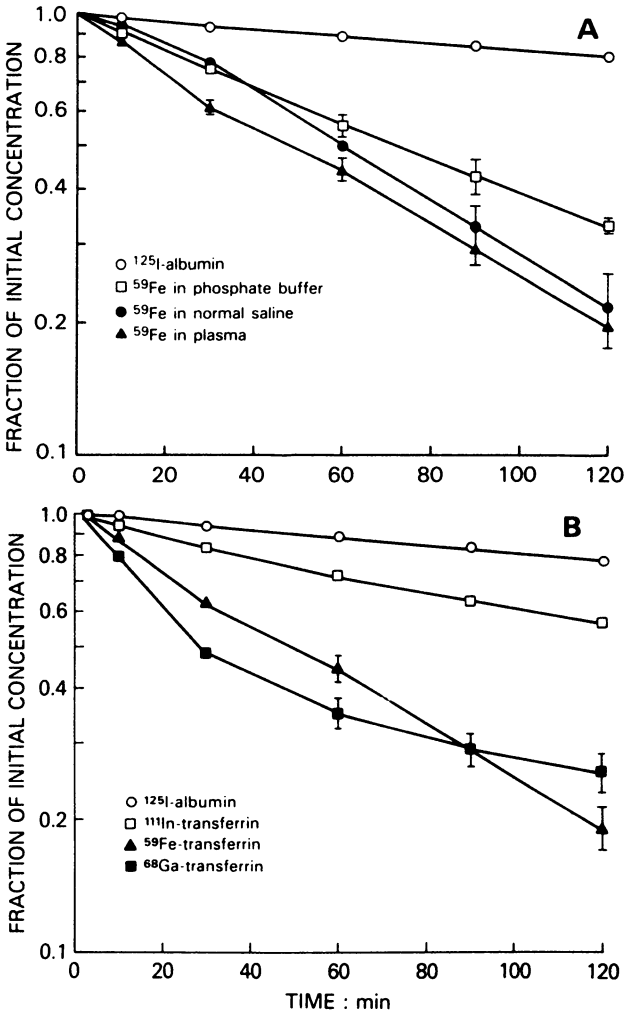

FIGURE 1
Plasma clearance. Each data point represents the mean ± s.e.m. of all individual animal values for each experimental group; the albumin values reflect all animals. A: Plasma clearance of three iron preparations [Fe1]: [$^{59}Fe^{++}$]citrate in phosphate buffer (pH = 7.0). [Fe2]: [$^{59}Fe^{++}$]citrate in normal saline. [Fe3]: [$^{59}Fe^{++}$]citrate in plasma. B: Plasma clearance of ^{59}Fe, ^{111}In, and ^{68}Ga. [Fe]: [^{59}Fe]citrate. [In]: [^{111}In]chloride. [Ga]: [^{68}Ga]chloride.

Experiment 1. The plasma clearance of [^{59}Fe] and [^{125}I] albumin could be fitted to a single exponential component (Fig. 1A). The arterial plasma clearance of ^{59}Fe was more rapid than [^{125}I]albumin for each of the Fe preparations ($p < 0.01$). The plasma half-life for [Fe1], [Fe2], and [Fe3] was 70 ± 10, 53 ± 8 and 49 ± 4 min (means ± s.e.m.), respectively. There was no statistical difference between the three ^{59}Fe preparations. In vivo binding of ^{59}Fe to plasma proteins (transferrin) and the stability of intravascular [^{125}I]albumin were determined by ultrafiltration; the nonfiltered fraction of ^{59}Fe and ^{125}I in the 1, 10, and 120 min plasma samples was always more than 99% in all cases and no differences were found between preparations [Fe1], [Fe2], and [Fe3]. The extent of ^{59}Fe and ^{125}I uptake by red blood cells (C_{rbc}) during the 120 min experiments was determined. At 1 and 10 min after injection, virtually all the radioactivity in whole blood was confined to the plasma compartment. At the end of the experiment (120 min), a sizable and variable fraction of ^{59}Fe radioactivity was found in red blood cells; the C_{rbc}/C_p ratios for preparations [Fe1], [Fe2], and [Fe3] were 0.41 ± 0.27, 1.73 ± 0.85, and 1.92 ± 2.03 (means ± s.d.), respectively. Iodine-125 radioactivity remained in the plasma compartment throughout the experiment.

The distribution spaces of ^{59}Fe in various tissues were significantly higher than those of albumin irrespective of the iron preparation (Fig. 2A and B, Table 2). The DS(iron)/DS(albumin) ratios of the [Fe3] preparation in heart, kidney, and muscle were smaller than those of the [Fe1] preparation, while, in brain, liver and spleen, those of the [Fe3] preparation were larger than the [Fe1] preparation. In spleen the distribution spaces varied considerably for each iron preparation; values ranged from 0.437 to 5.12. Although the [Fe2] preparation showed a tendency toward large distribution spaces, there was considerable variability between animals and the differences between different preparations were significant only in brain with respect to [Fe1], and in heart and kidney with respect to [Fe3].

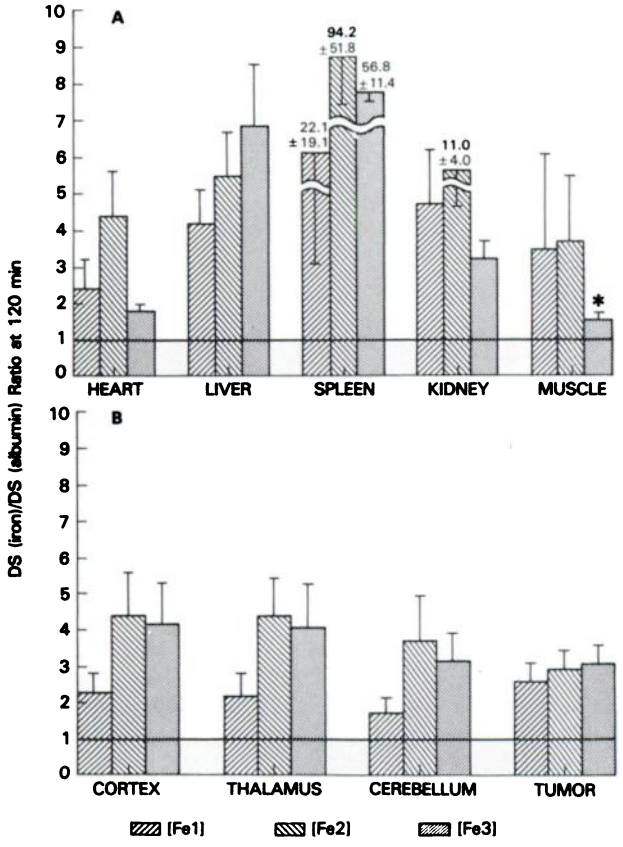

FIGURE 2
Ratios of iron and albumin distribution spaces at 120 min. [Fe1]: [$^{59}Fe^{++}$]citrate in phosphate buffer (pH = 7.0). [Fe2] : [$^{59}Fe^{++}$]citrate in normal saline. [Fe3]: $^{59}Fe^{++}$ citrate in plasma. Values are the mean ± s.d. All values were significantly greater than 1.0 ($p < 0.01$, except "*" where $p < 0.05$; paired t-test). A: Systemic organs. B: Brain.

TABLE 2
Albumin Distribution Spaces (ml/g)

Organs	30 min n = 17	120 min n = 33
Heart	0.101 ± 0.018	0.124 ± 0.015
Lung	0.205 ± 0.116	0.221 ± 0.089*
Liver	0.091 ± 0.010	0.092 ± 0.025
Spleen	0.081 ± 0.010	0.081 ± 0.020
Kidney	0.059 ± 0.012	0.072 ± 0.013
Muscle	0.010 ± 0.006	0.013 ± 0.006
Cortex	0.007 ± 0.002	0.008 ± 0.001
Thalamus	0.007 ± 0.001	0.008 ± 0.002
Cerebellum	0.015 ± 0.003	0.016 ± 0.003
Tumor	0.057 ± 0.015	0.122 ± 0.26

Values are the means ± s.d.
*n = 21.

The intracerebral Walker-256 tumor developed around the injection site and was confined within the right cerebral hemisphere. The left cerebral hemisphere appeared normal without evidence of brain swelling. The distribution space of iron in the brain tumor was considerably higher than the albumin space of the tumor ($p < 0.01$) (Fig. 2B).

Experiment 2. The plasma clearance curve of ^{111}In and ^{68}Ga was biexponential, while ^{59}Fe and [^{125}I]albumin could be fitted to a single exponential (Fig. 1B). The half-life of the second component for ^{111}In and ^{68}Ga was 232 ± 93 and 157 ± 43 min (mean ± s.e.m.), respectively, and represented 90% and 46%, respectively, of injected radioactivity as determined by the initial (1 min) plasma level, respectively. The plasma half-life for ^{59}Fe and [^{125}I]albumin was 49 ± 4 and 297 ± 97 min, respectively (Fig. 1B). The ^{59}Fe and ^{68}Ga half-lives were significantly shorter than albumin, while the second component of ^{111}In clearance was similar to that of albumin.

In vivo binding of ^{59}Fe, ^{111}In, and ^{68}Ga to plasma proteins (transferrin) and the stability of [^{125}I]albumin were determined by ultrafiltration; the retention fraction of ^{59}Fe, ^{111}In, ^{68}Ga, and ^{125}I in the 1, 10, 30, and 120 min plasma samples was always more than 99% in all cases. Indium, gallium and iodine radioactivity in all blood samples was essentially within the plasma compartment during the 30 and 120 min experiments, while substantial iron radioactivity was found in the red blood cell compartment. The 30 and 120 min C_{rbc}/C_p ratio for the iron preparation was 0.21 ± 0.15 and 1.92 ± 2.03 (means ± s.d.), respectively.

The distribution spaces of iron, indium and gallium were compared to albumin spaces using DS(metal)/DS(albumin)

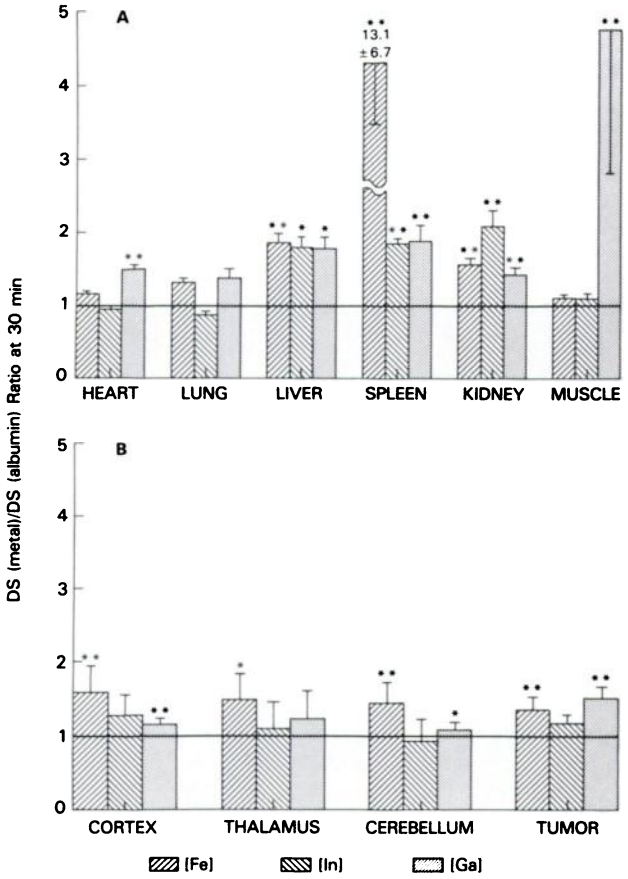

FIGURE 3
Ratios of metal and albumin distribution spaces at 30 min. [Fe]: [^{59}Fe]citrate. [In]: [^{111}In]chloride. [Ga]: [^{68}Ga]chloride. Values are the mean ± s.d. Significant differences between the metal and albumin spaces. *: $p < 0.05$, **: $p < 0.01$; paired t-test.

ratios for the 30 and 120 min experiments (Table 2, Fig. 3A and B, Fig. 4A and B). Among the three transferrin-metal chelates studies, indium showed a tendency toward smaller ratios among the three metals. The tissue spaces of gallium and iron 120 min after injection were always larger than the albumin spaces and the 120 min iron spaces showed the largest differences compared to albumin. Large differences in the metal-chelate distribution spaces were found in liver, spleen and kidney regardless of the preparation. In spleen, the iron distribution spaces varied considerably as mentioned above, whereas the individual indium and gallium spaces in the same organs did not vary much. The 30-min experiments showed the same tendency as the 120-min experiments.

Indium spaces were the same as those measured with albumin in heart, lung, muscle, cerebellum and brain tumor (Figs. 3 and 4). In lung the albumin distribution spaces showed large variability (Table 2), reflecting random sampling of congested (blood-filled) and noncongested tissue in different animals. In liver and spleen the indium distribution space at 120 min was larger than that of gallium, but less than that of iron. In parietotemporal cortex and thalamus, the indium spaces 120 min after injection were larger than albumin, however, the magnitude of these differences were small. For cortex and thalamus, the DS(indium)-DS(albumin) difference was 0.0017 and 0.0024 ml/g, respectively (Fig. 5). At 30 min, indium spaces in brain were the same as those of albumin.

Gallium accumulated in muscle to a considerably large degree in comparison to indium and iron in both the 30 and 120 min experiments. With the exception of muscle, tissue distribution of ^{68}Ga was similar to that of ^{111}In with the tendency toward larger distribution spaces. The differences with respect to albumin were significant for all tissues sampled.

For the intracerebral Walker-256 tumor, the indium space showed the same value as albumin at both 30 and 120 min. The iron and gallium spaces in the tumor were larger than the albumin space at both 30 and 120 min (Fig. 3B, 4B). At 120 min the distribution space of brain tumor was more than tenfold larger than that of the contralateral normal brain irrespective of the preparation.

DISCUSSION

We have examined [^{59}Fe]citrate, [^{111}In]chloride and [^{68}Ga]chloride labeling of the plasma metal binding protein transferrin for use as a potential marker of vascular permeability. In a previous study of gallium-transferrin chelates, we demonstrated relative instability of the gallium-transferrin complex in vivo that preclude

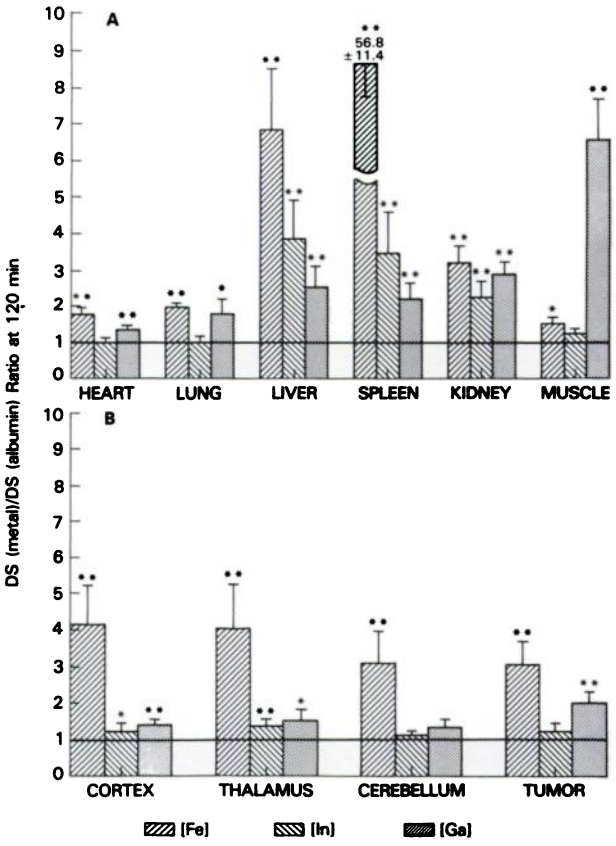

FIGURE 4
Ratios of metal and albumin distribution spaces at 120 min. [Fe]: [^{59}Fe]citrate. [In]: [^{111}In]chloride. [Ga]: [^{68}Ga] chloride. Values are the mean ± s.d. Significant differences between the metal and albumin spaces. *: $p < 0.05$, **: $p < 0.01$; paired t-test. A: Systemic organs. B: Brain.

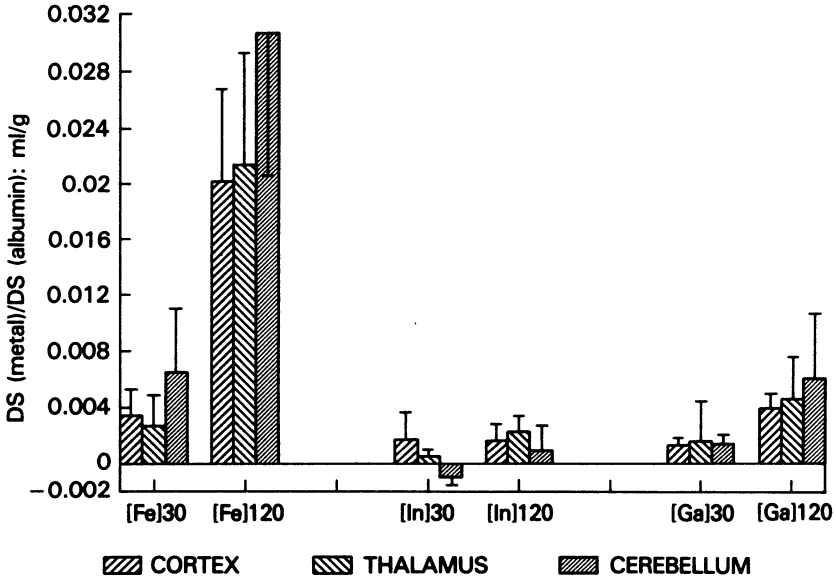

FIGURE 5
Differences between the metal and albumin distribution spaces at 30 and 120 min. [Fe]: [^{59}Fe]cigrate. [In]: [^{111}In]chloride. [Ga]: [^{68}Ga]chloride. Values are the mean ± s.d.

its use as an acceptable radiolabeled macromolecule for vascular permeability studies using PET scanning techniques (*4*). Since transferrin chelates several metals with high affinity, we elected to study ferrous citrate and indium chloride as well. Both metals have useful gamma-emitting radionuclides (^{59}Fe and ^{111}In) as well as positron emitting radionuclides (^{52}Fe and ^{110}In) that can be produced by a cyclotron and are suitable for PET scanning. Indium has similar chemical properties to gallium since both elements are in the same group (IIIA) of the periodic classification of the elements. Although iron is not a group IIIA element, there are many aspects of its chemistry which resemble those of gallium and indium (*11*). In acidic solution, iron, indium and gallium in the +3 oxidation state exist as octahedrally coordinated cations. When the pH of the solution is raised, all three metals hydrolyze leading to neutral trihydroxide precipitates. To avoid the formation of radiocolloid precipitates which are pharmaceutically inactive in aqueous solution, these radiometals are commercially available only in highly acidic solutions such as hydrochloric and citric acids.

Ideally, transferrin-bound radionuclide should be injected in the form which is found naturally in plasma. For example, the link between iron and transferrin is strictly pH-dependent, and the binding of iron is complete only above pH 7.0, and dissociation begins below pH 6.5 (*12*). However, ferric salts at neutral pH tend to form insoluble hydroxides. Previous reports, investigating the effect of pH on the formation of the iron-transferrin complex could not exclude the formation of hydroxides after rapid neutralization to physiologic pH by the buffering action of blood (*13*). This presents problems in the formulation of a transferrin bound metal.

As iron has a much higher stability constant for binding to transferrin than gallium and indium ions (*12*), we have examined iron citrate for the labeling of the autologous protein, transferrin. Ferrous ion, in citric acid, is a convenient formulation since it can be readily used to study the effect of diluents and can be neutralized with phosphate buffer or plasma without forming precipitates. The maximum solubility of Fe^{3+} at pH 7.0 is 10^{-17} mol/l, whereas that of Fe^{2+} is considerably higher, 10^{-1} mol/l (5.9 mg/ml) (*14*). Although iron is complexed by transferrin in the ferric form, ferrous iron added to plasma binds more completely than ferric iron (*15*).

Three diluents (phosphate buffer, saline and plasma) of the [$^{59}Fe^{++}$]citrate stock solution were compared. The equivalent amount of iron in 1 ml of the resultant dilution was 1.2×10^{-3} mg (25 mCi/mg Fe); this concentration is well below the solubility of ferrous ion in aqueous solution at neutral pH. Therefore, radioactive $^{59}Fe^{++}$ in citrate could be neutralized without forming hydroxide precipitates. After injection of Fe^{++} citrate, normal homeostatic control of the redox potential in biological fluids such as plasma appears to be sufficient to result in a rapid oxidation of Fe^{++} to biologically active Fe^{+++} and a rapid binding to transferrin (*14*). The copper protein ceruloplasmin, and perhaps other serum ferroxidases, may play an essential role in the oxidation of ferrous ion and result in a much faster oxidation than expected from the redox potential of plasma alone (*15*). The in vitro and in vivo changes of iron preparations are illustrated in Figure 6.

We suggest that the [Fe3] preparation yielded the "best" results with respect to iron-transferrin complex formation in vivo. The [Fe3] preparation showed a tendency for the lowest DS(iron)/DS(albumin) ratios in systemic organs, while in brain [Fe3] had the highest DS ratios of the three iron preparations studied. The higher iron spaces in brain with the [Fe3] preparation may be due to a higher fraction of "optimal" iron

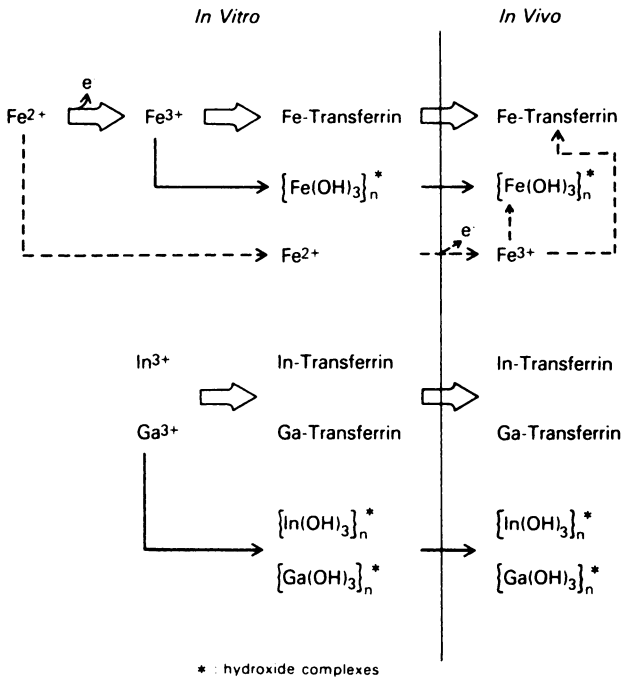

FIGURE 6
Schematic of metal-plasma interaction, in vitro and in vivo.

transferrin complexes, such as diferric ([^{59}Fe]$_2$)-transferrin, for binding to transferrin receptors on brain and endothelium (*16*) and transport across the blood brain barrier. Transferrin receptors have not been identified on the endothelial cells in systemic organs, other than liver and bone marrow (*15*). In systemic organs, radiolabeled iron complexes can be transported across the capillaries by diffusion and convection, and can move in various forms such as monoferric-transferrin and iron hydroxides. Although the [Fe2] preparation is simple and widely used, our results showed such variable distribution spaces among individual animals that we considered the [Fe2] preparation unacceptable.

Previously we tested three gallium-plasma preparations; all three gave similar blood clearance and tissue distribution data suggesting instability of the gallium-transferrin complex in vivo (*4*). The results of Vallabhajosula (*17*) and Weiner (*18*) support this observation in that they demonstrate instability of the gallium-transferrin complex under various in vitro conditions. Although the role of different anions (oxalate, malonate, nitrilotriacetate) in the formation of gallium-transferrin complexes and their effects on tumor uptake have been evaluated (*19*), bicarbonate is the critical anion involved in the formation of metal-transferrin complexes in vivo. For example, Hammersley et al. (*20*) demonstrated in vivo that gallium biodistribution is independent of citrate concentration.

We did not perform electrophoresis to analyze our metal-chelate preparations for reasons previously discussed (*21*). Gel filtration and column chromatography was applied to three gallium-chelate preparations and the results were shown to be highly dependent on the choice eluants and solvents, respectively (*4*). Therefore, we chose the comparatively simple ultrafiltration system to test for large molecular weight complex formation (30,000 D) of both the in vitro preparations and the in vivo plasma samples obtained at various times after injection.

Comparison of Iron, Indium, and Gallium

The nonprotein bound fraction of the three metals in plasma was either small or the metal complexes were of high molecular weight since the nonfiltered fraction 1 min after i.v. injection was only 1% or less. Nevertheless, the plasma clearances of three metal chelates were quite different. Only the half-life of the second exponential component of indium was similar to that of albumin. A previous study reported a faster plasma clearance of indium, but did not take into account the initial, more rapid phase of indium clearance that we observed (*22*). This rapid phase, accounting for only 10% of injected radioactivity, may be due to renal excretion of nonprotein bound indium in the injectate and reflected in the comparatively high distribution space of indium in kidney at 30 min.

Incorporation of radioactivity in red blood cells was observed only with iron. Indium-111 chloride was initially introduced for bone marrow imaging (*23*), since it was transported to bone marrow and taken up by reticulocytes in a manner similar to iron. However, the percent uptake of indium was much less than iron, and indium uptake by matured red cells was demonstrated to be minimal (*24*). No indium was found in the red blood cell fraction 120 min after i.v. injection of the indium-transferrin complex in our experiments; this corroborates the finding of other workers (*22*). Indium, like albumin and gallium, is confined to the plasma fraction during the first hours after injection. The sizable but variable amount of radiolabeled iron incorporated into red blood cells during our experiments resulted in an apparent increase in the tissue distribution space and a correction for red blood cell radioactivity in the case of iron was necessary.

Although iron, gallium, and indium were complexed to the plasma protein transferrin and transported in plasma in a similar fashion, marked differences in the distribution of the three metals in various organs were noted. One notable difference was the significantly higher distribution space of iron in brain compared to that of indium and gallium; these differences will be discussed later with respect to transferrin receptor mediated endocytosis (*15,16*). In liver and spleen, where active iron turnover take place, iron distribution spaces were highest.

The indium spaces in heart, lung, muscle, Walker-256 allografts and brain were the same or very close to that of albumin. This suggests that the indium-transferrin complex may be a more useful macromolecular

tracer for studying the vascular permeability of these organs. In the rat, the indium-transferrin complex appears to be a better macromolecular tracer than the gallium complex for measuring vascular permeability in the lung (Figs. 3A and 4A). However, Gorin (*25*) has reported a substantially higher transcapillary escape rate of [^{113}In]transferrin in comparison to [^{131}I]albumin in humans, and the indium values were similar to the gallium values reported by Mintun et al. (*6*). A steady increase in the indium distribution space was observed between 30 and 120 min in liver and spleen; it probably does not represent an uptake or clearance of nonprotein bound indium.

Gallium showed a remarkable feature by accumulating in muscle to a substantially greater degree than either indium or iron. This was clearly apparent in both the 30 and 120 min experiments. Sephton et al. also observed a similar phenomenon in a set of tumor-bearing mice (*26*). The vascular endothelium of skeletal muscle is characterized by capillaries with small pores that restrict the diffusion of modest-size plasma solutes across the capillary (*27,28*). The relatively high concentration of gallium in muscle tissue compared to albumin, iron, and indium could reflect an active transport mechanism for gallium-transferrin or the diffusion of gallium hydroxides across muscle capillaries. Hayes et al. showed that an increase in plasma protein binding of ^{67}Ga would increase the uptake of ^{67}Ga in soft tissues, suggesting the preferential transport of gallium-transferrin across the muscle capillary wall in comparison to nontransferrin complexes of gallium (*29*).

Receptor Mediated Endocytosis of Transferrin

Virtually no passive diffusion or transport across normal brain capillaries is expected for proteins with a molecular size of albumin or transferrin. Even hydroxide complexes of the smallest possible molecular size at physiological pH, such as $^{59}Fe(OH)_3$, $^{111}In(OH)_3$, and $^{68}Ga(OH)_3$, could not readily diffuse across the blood-brain barrier (*30*). This property provides an excellent experimental model for studying the recently identified transferrin receptor on brain capillaries (*31*). If the transferrin receptors in brain capillaries mediate the transport of these metal chelates into the brain, this data suggests that indium-transferrin has a low affinity to the transferrin receptor in comparison to iron-transferrin and that the affinity of gallium-transferrin to the receptor is somewhat intermediate. The rank order of transported iron and gallium at 120 min was cerebellum $>$ thalamus $\geq$ cortex, which is in accordance with the number of transferrin receptors reported for these brain regions (*31*). This suggests that by using iron- or gallium-transferrin, the distribution and quantification of transferrin receptors in brain endothelium might be estimated and visualized in vivo.

Receptor affinity for transferrin in rat brain appears indistinguishable from transferrin receptors previously characterized in other tissues (*31,32*). However, the metal exerts an important effect on the transferrin molecule and its affinity to the transferrin receptor. Diferric transferrin has the highest affinity, monoferric transferrin intermediate affinities, and apotransferrin has very little affinity at physiologic pH of 7.4 (*33*). These differences can be related to a conformational change of the transferrin molecule when it chelates to one or two ferric ions (*12*). Based on these observations, we suggest that there may be different affinities to the transferrin receptor for the iron-, indium- and gallium-transferrin complexes in vivo. The ionic radii (*34*) of iron (0.064 nm), and gallium (0.062 nm) are similar; both iron and gallium spaces in brain were larger than albumin spaces, although the two transferrin chelates appear to have different affinities to the transferrin receptor. The ionic radius of indium (0.081 nm) is considerably larger than those of iron and gallium, and a conformational change in transferrin after chelation with indium could result in lowering its affinity to the receptor, resulting in the observed similarity between indium and albumin spaces in brain.

A conformational difference between the transferrin-metal chelates, resulting in different affinities to the transferrin receptor, does not explain all our in vivo distribution data. Skeletal muscle capillaries are relatively impermeable to molecules the size of albumin and transferrin (Table 2) (*27,28*). In skeletal muscle, a pattern opposite to that observed in brain was observed; gallium spaces were significantly larger than iron spaces, which were similar or only slightly larger than those of indium and albumin (Fig. 3A, 4A). Panaccio et al. have suggested a heterogeneity of the human transferrin receptor from their studies of different malignant cell lines (*35*). Our data suggest that iron and gallium transport across vascular endothelium may be influenced by factors other than the affinity of the metal-transferrin complex to the transferrin receptor or that a subclass of the transferrin receptor exists in different endothelial cells with different affinities to different metal-transferrin complexes.

Transport and Transferrin Receptors in Tumors

The movement of macromolecules such as transferrin and albumin across the capillaries of tumors and normal tissue parenchyma can occur by diffusion and convection through fairly large size "pores" or "channels" that exist between or through endothelial cells (*10*). However, receptor mediated endocytosis can be another mechanism for passage across vascular endothelium (e.g., brain) and through cell membranes. Transferrin receptor in measurable numbers exist in many body tissues. They are especially abundant in erythrocyte precursors, placenta and liver. In malignant tissue the transferrin receptor is in higher concentration than in benign lesions (*36,37*). Recent studies show that proliferation of various cell types involves the regulation

of transferrin, its receptor and the entry of iron into the cell (*38,39*), and that an abundance of transferrin receptors is at the surface of certain malignant tumor cells. The two- to threefold higher levels of gallium and iron in comparison to albumin in Walker-256 intracranial allografts 120 min after injection of the metal-transferrin chelate corroborates previously reported observations; these metal complexes are taken up by or bound to tumors (*29,36,37*). Indium-labeled transferrin has also been used for the detection of tumors (*40*). Our results demonstrate that indium accumulation by tumor tissue was tenfold larger than normal brain regions at 120 min, however, little or no specific tumor uptake of the indium complex was observed since the DS(indium)/DS(albumin) ratio approximates unity. Indium-transferrin can be used to measure vascular permeability and the distribution of transferrin in the extracellular space of Walker-256 tumors.

CONCLUSIONS

The clinical implications of these studies lead in several directions. For in vivo studies related to the transferrin receptor, iron-transferrin appears to have a selective advantage for erythroid precursor cells, malignant tumors and brain, whereas gallium-transferrin may be preferential for tissue such as skeletal muscle. A control measurement to account for passive distribution of the macromolecule across the capillaries, using albumin or indium-transferrin, will be required to quantitate or image specific receptor binding and iron incorporation. Of the three metal-transferrin chelates, the indium complex appears best for measuring vascular permeability of tumors, heart, lung and skeletal muscle; the transferrin macromolecule has a hydrodynamic diameter which is close to that of albumin and Fab fragments (*1,2*).

Clinical studies can be performed using PET; ^{110}In could be used to label plasma transferrin and evaluate vascular permeability, and ^{52}Fe could be used in the evaluation and imaging of transferrin receptors. The role for gallium is less clear; if subtypes of the transferrin receptor are found with preferential affinity for the gallium-transferrin complex, its usefulness may increase.

ACKNOWLEDGMENTS

The support and helpful suggestions of Dr. Steven Larson are gratefully acknowledged and the excellent secretarial assistance of Ms. Juli Maltagliati is appreciated.

REFERENCES

1. Rosseneu-Motoreff MY, Soetewey F, Lamote R, et al. Size and shape determination of apotransferrin and transferrin monomers. *Biopolymers* 1971; 10:1039–1048.
2. Edsall JT. The size, shape and hydration of protein molecules. In: Neurath H, Bailey K, eds. *The protein.* New York: Academic Press; 1953:549–726.
3. Blasberg RG, Nakagawa H, Bourdon MA, Groothuis DR, Patlak CS, Bigner DD. Regional localization of a glioma associated antigen defined by monoclonal antibody 81C6 *in vivo*. *Cancer Res* 1987; 47:4432–4443.
4. Brunetti A, Blasberg RG, Finn RD, Larson SM. Gallium transferrin as a macromolecular tracer of vascular permeability. *Nucl Med Biol* 1988; 15:665–672.
5. Gorin AB, Kohler J, DeNardo G. Noninvasive measurement of pulmonary transvascular protein flux in normal man. *J Clin Invest* 1980; 66:869–877.
6. Mintun MA, Dennis DR, Welch MI, Mathias CJ, Schuster DP. Measurement of pulmonary vascular permeability with PET and gallium-68 transferrin. *J Nucl Med* 1987; 28:1704–1716.
7. Sayle BA, Balachandran S, Rogers CA. Indium-111 chloride imaging in patients with suspected abscesses. *J Nucl Med* 1983; 24:1114–1118.
8. Iles SE, Ehrlich LE, Saliken JC, Martin RH. Indium-111 chloride scintigraphy in adult osteomyelitis. *J Nucl Med* 1987; 28:1540–1545.
9. Hiraga S, Klubes P, Owens ES, Cysyk RL, Blasberg RG. Increases in brain tumor and cerebral blood flow by blood-perfluorochemical emulsion (Fluosol-DA) exchange. *Cancer Res* 1987; 47:3296–3302.
10. Nakagawa H, Groothuis DR, Owens ES, Fenstermacher JD, Patlak CS, Blasberg RG. Dexamethasone effects on [^{125}I] albumin distribution in experimental RG-2 gliomas and adjacent brain. *J Cereb Blood Flow Metab* 1987; 7:687–701.
11. Moerlein SM, Welch MJ. The chemistry of gallium and indium as related to radiopharmaceutical production. *Int J Nucl Med Biol* 1981; 8:277–287.
12. Aisen P. The transferrins. In: Jacobs A, Worwood M, eds. *Iron in biochemistry and medicine 2.* London: Academic Press; 1980:87–129.
13. Kulprathipanja S, Hnatowich DJ, Evans G. The effect of pH on the *in vivo* and *in vitro* behavior of complex-free ^{68}Ga and ^{113m}In. *Int J Nucl Med Biol* 1979; 5:140–144.
14. May PM, Williams DR. The inorganic chemistry of iron metabolism. In: Jacobs A, Worwood M, eds. *Iron in biochemistry and medicine 2.* London: Academic Press; 1980:1–28.
15. Huebers HA, Finch CA. The physiology of transferrin and transferrin receptors. *Physiol Rev* 1987; 67:520–582.
16. Jefferies WA, Brandon MR, Hunt SV, Williams AF, Gatter KC, Mason DV. Transferrin receptor on endothelium of brain capillaries. *Nature* 1984; 312:162–163.
17. Vallabhajosula SR, Harwig JF, Wolf W. The mechanism of tumor localization of gallium-67 citrate: role of transferrin binding and effect of tumor pH. *Int J Nucl Med Biol* 1981; 8:363.
18. Weiner RE. Role of phosphate-containing compounds in the transfer of indium-111 and gallium-67 from transferrin to ferritin. *J Nucl Med* 1989; 29:70–79.
19. Terner UK, Noujaim AA, Lentle BC, Turner CJ. The effects of differing gallium-transferrin-anion complexes on the tumor uptake of gallium-67. *Int J Nucl Med Biol* 1981; 8:357–362.
20. Hammersley PAG, Zivanovic MA. The relationship

of ^{67}Ga uptake to citrate dose, compared with ^{67}Ga-chloride and ^{67}Ga-transferrin in rodent tissues and tumours. *Nucl Med* 1980; 19:25.
21. Vallabhajosula SR, Harwig JF, Wolf W. Radiogallium localization in tumors: blood binding and transport and the role of transferrin. *J Nucl Med* 1980; 21:650.
22. Nahmias C, Ikeno C, Coates G. Can indium-113m be used to measure the transcapillary escape rate of transferrin? *Microvasc Res* 1981; 21:128–132.
23. Lilien DL, Berger HB, Anderson DP, Bennett LR. ^{111}In-chloride: a new agent for bone marrow imaging. *J Nucl Med* 1973; 14:184–186.
24. Adatepe MH, Penkoske P, van Amberg A, Wharton T, Evens RG, Potchen EJ. Red cell and plasma protein labeling with ^{113m}In. *Int J Appl Radiat* 1971; 22:498–501.
25. Gorin AB. External radio-flux detection: noninvasive measurement of protein leakage in assessing lung microvascular injury. *Ann NY Med Sci* 1982; 384:411–416.
26. Sephton RG, De Abrew S, Hodgson GS. Mechanisms of distribution of gallium-67 in mouse tumor hosts. *Br J Radiol* 1982; 55:134–141.
27. Firrell JC, Lewis GP, Youlten LTF. Vascular permeability to macromolecules in rabbit paw and skeletal muscle. *Microvasc Res* 1982; 23:294–310.
28. Sejrsen P, Paaske WP, Henriksen O. Capillary permeability of ^{131}I-albumin in skeletal muscle. *Microvasc Res* 1985; 29:265–281.
29. Hayes RL, Rafter JJ, Byrd BL, Carlton JE. Studies of the *in vivo* entry of Ga-67 into normal and malignant tissue. *J Nucl Med* 1981; 22:325–332.
30. Fenstermacher JD, Rapoport SI. Blood-brain barrier. In: Renkin EM, Michel CC, eds. *Handbook of physiology*. Bethesda: American Physiological Society; 1984:969–1000.
31. Hill JM, Ruff MR, Weber RJ, Pert CB. Transferrin receptors in rat brain. *Proc Natl Acad Sci USA* 1985; 82:4553–4557.
32. Dautry-Versat A, Lodish HF. How receptors bring protein and particles into cells. *Sci Am* 1984; 250:52–58.
33. Huebers HE, Csiba E, Huebers E, Finch CA. Competitive advantage of diferric transferrin in delivering iron to reticulocytes. *Proc Natl Acad Sci USA* 1983; 80:300–304.
34. Shannon RD. Revised effective ionic radii and systemic studies of interatomic distances. *Acta Crystallogr* 1976; A32:751–767.
35. Panaccio M, Zalcberg JRT, Thompson CH, et al. Heterogeneity of the human transferrin receptor and use of anti-transferrin receptor antibodies to detect tumors *in vivo*. *Immunol Cell Biol* 1987; 65:461–472.
36. Bomford AB, Munro HN. Transferrin and its receptor. *Hepatology* 1985; 5:870–875.
37. Faulk WP, Hsi BL, Stevens PJ. Transferrin and transferrin receptors in carcinoma of the breast. *Lancet* 1980; 2:390–392.
38. Larson SM, Rasey JS, Allen DR, Nelson SJ. A transferrin-mediated uptake of gallium-67 by EMT-6 sarcoma. *J Nucl Med* 1979; 20:837–842.
39. Harding C, Heuser J, Stahl P. Receptor mediated endocytosis of transferrin and recycling of the transferrin receptor in rat reticulocytes. *J Cell Biol* 1983; 97:329–339.
40. Goodwin DA, Goode R, Brown R, Imbornone CJ. ^{111}In-labeled transferrin for the detection of tumor. *Radiology* 1971; 100:175–179.